



Research paper

## A Novel Method for Medical Image Segmentation Based on Convolutional Neural Networks with SGD Optimization

M. Taheri<sup>1,\*</sup>, M. Rastgarpour<sup>2</sup>, A. Koochari<sup>1</sup>

<sup>1</sup>Department of Computer Engineering, Faculty of Engineering, Islamic Azad University, Science and Research Branch, Tehran, Iran.

<sup>2</sup>Department of Computer Engineering, Faculty of Engineering, Islamic Azad University, Saveh Branch, Saveh, Iran.

### Article Info

#### Article History:

Received 10 May 2020

Reviewed 01 July 2020

Revised 08 September 2020

Accepted 12 November 2020

#### Keywords:

Deep learning

Convolutional neural networks

Medical image segmentation

Image processing

Computer vision

\*Corresponding Author's Email Address:

[mohammad-taheri@srbiau.ac.ir](mailto:mohammad-taheri@srbiau.ac.ir)

### Abstract

**Background and Objectives:** medical image Segmentation is a challenging task due to low contrast between Region of Interest and other textures, hair artifacts in dermoscopic medical images, illumination variations in images like Chest-Xray and various imaging acquisition conditions.

**Methods:** In this paper, we have utilized a novel method based on Convolutional Neural Networks (CNN) for medical image Segmentation and finally, compared our results with two famous architectures, include U-net and FCN neural networks. For loss functions, we have utilized both Jaccard distance and Binary-crossentropy and the optimization algorithm that has used in this method is SGD+Nestrov algorithm. In this method, we have used two preprocessing include resizing image's dimensions for increasing the speed of our process and Image augmentation for improving the results of our network. Finally, we have implemented threshold technique as postprocessing on the outputs of neural network to improve the contrast of images. We have implemented our model on the famous publicly, PH2 Database, toward Melanoma lesion segmentation and chest Xray images because as we have mentioned, these two types of medical images contain hair artifacts and illumination variations and we are going to show the robustness of our method for segmenting these images and compare it with the other methods.

**Results:** Experimental results showed that this method could outperformed two other famous architectures, include U-net and FCN convolutional neural networks. Additionally, we could improve the performance metrics that have used in dermoscopic and Chest-Xray segmentation which used before.

**Conclusion:** In this work, we have proposed an encoder-decoder framework based on deep convolutional neural networks for medical image segmentation on dermoscopic and Chest-Xray medical images. Two techniques of image augmentation, image rotation and horizontal flipping on the training dataset are performed before feeding it to the network for training. The predictions produced from the model on test images were postprocessed using the threshold technique to remove the blurry boundaries around the predicted lesions.

©2021 JECEI. All rights reserved.

### Introduction

Medical image segmentation is one of the most

important and vital tasks that in recent years, many computer-based procedures have developed to do this

task precisely. Likewise, in this paper we have introduced an algorithm for automatic medical image segmentation toward segmenting melanoma cancer images and Chest-Xray medical images.

Actually, this important and vital task contains the process of automatic or semi-automatic detection of boundaries within a 2D or 3D image. A major difficulty of this task is the high variability in medical images. First of all, human's anatomy and body's organs include lots of variations in each person. After that, different imaging modalities (X-ray, CT, MRI, Microscopy, PET, SPECT, Endoscopy, OCT, and etc.) that use to create medical images from different organs of patients. As we have mentioned before, there are some problems in medical images such as hair artifacts in dermoscopic medical images and the images which are related to the hairy parts of body. Segmentation task in medical images resulted in separate the region of interest (ROI) from other regions that exist in different medical images. This task helps doctors for further diagnostic insights and cure the patients. Possible applications are automatic measurement of organs, cell counting, or simulations based on the extracted boundary information.

This paper is organized as following. first, we discuss about previous works in section II, then we introduce the details of the proposed segmentation method in Section III, then report the experimental design and results in Section IV. Finally, we conclude our study in Section V.

## Previous Works

In the past years, researches introduced many computer-based algorithms to solve medical image segmentation problem. Some of these efforts include:

Kim.J.U in [1], proposed an iterative structure in deep neural networks for medical image segmentation. in this method an encoder-decoder structure mixed with iterative structure until they can improve the segmentation results that include complex shapes in medical images. they utilized two technics include transfer-learning and data augmentation for prevent overfitting.

Chang.Y in [2], proposed a method for segmenting cardiac medical images. first of all, ROI detects by YOLO neural network then it feeds to a convolutional neural network for segmentation. finally, by a fully connected neural network, the segmented images classify and then the doctor can detect the type of cardiac disease precisely.

Isin in [3], discussed about different methods for brain image segmentation. these methods divide to three categories include: non-automatic, semi-automatic and automatic methods. In automatic methods, there is no intervention from human and because of this the probability of error decreases.

Pim in [4], could train a CNN for segmenting six

texture in MRI brain images, Chest muscle in muscle MRI images and vessel in CT cardiac images. then this method is suitable for segmentation of different organs and in different imaging conditions.

Dina Abdelhafiz in [5], proposed a method by Unet neural networks for addressing the lesions that exist in mammogram images precisely. In this paper, the accuracy improved, by batch normalization and data augmentation.

Hauzhu Fu in [6], developed a method for eye vessels segmentation by fully connected neural networks. this network produces the feature map of eye vessels and feeds it to CRF neural network until produces the binary images of eye vessels.

Zhe Gou in [7], analysed medical images in different levels include: feature learning, classifier level and decision making. They developed a neural network until detect malignant tumors in different imaging conditions (computerized tomography, PET and MRI).

Celebi et al in [8], used a procedure for skin lesion detection by using four threshold methods.

Zhou et al in [9], optimized the automatic skin lesion segmentation by mean shift estimation. This method needs many computational sequences.

Xie et al in [10], combined a neural network method with genetic algorithm for skin lesion segmentation.

Recently, convolutional neural networks are one of the most important and practical algorithms in the image segmentation task, specifically for medical image segmentation [11]. This algorithm has been used for brain tumor segmentation in MR brain images [12], cardiac image segmentation [13], skin lesion segmentation by non dermoscopic images [14] and many other medical image segmentation tasks which are related to different parts of the body with different shapes of organs and various artifacts.

## Proposed method

Stochastic Gradient Descent (SGD) is the optimization algorithm which has been used in this method. It is an iterative method for optimizing an objective function with suitable smoothness properties. It can be regarded as a stochastic approximation of gradient descent optimization, since it replaces the actual gradient by an estimate thereof. Especially in high dimensional optimization problems, it reduces the computational burden, achieving faster iterations in trade for a lower convergence rate. A good overview with convergence rates can be found in [15]. Given a set of training examples  $(x_1, y_1), \dots, (x_n, y_n)$  where  $x_i \in R^m$  and  $y_i \in R$  ( $y_i \in -1, 1$  for classification), our goal is to learn a linear scoring function  $f(x) = w^T x + b$  with model parameters  $w \in R^m$  and intercept  $b \in R$ . In order to make predictions for binary classification, we simply look at the sign of  $f(x)$ . To find the model parameters, we

minimize the regularized training error given by following formula:

$$E(w, b) = \frac{1}{n} \sum_{i=1}^n L(y_i, f(x_i)) + \alpha R(w) \quad (1)$$

In this method, there are two preprocess steps that have been done on medical images which feed to the network. These steps include resizing the images and image augmentation. After that, preprocessed images enter to the network for segmentation process. The outputs are segmented images which are blurred. We have solved this problem by a post processing step which uses threshold technique to make the segmented images sharper. We have shown the sequence of our algorithm in Fig. 1.

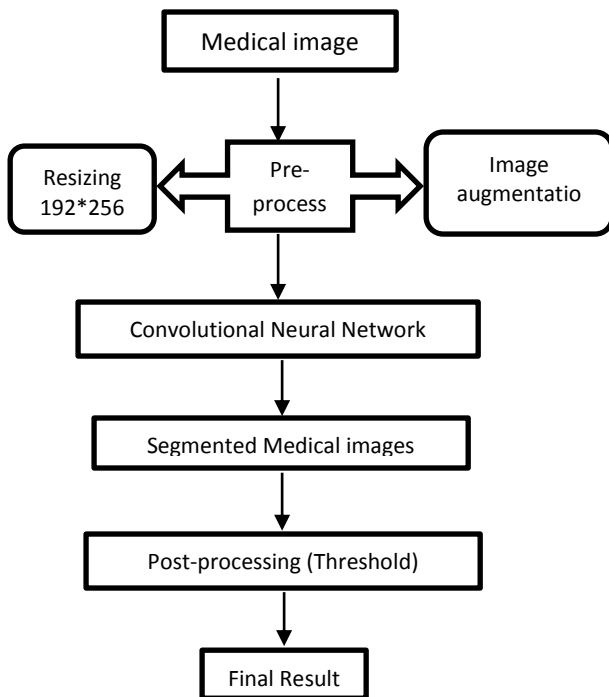


Fig. 1: The sequence of implemented algorithm.

#### A. Network Architecture

The proposed deep neural network contains an encoder decoder structure that includes 64-layer network excluding the final activation layer. Every sequence of encoder has multiple convolutional layers, batch normalized with ReLU nonlinearity which is followed by non-overlapping max pooling and sub-sampling. At the center of the network there are two dense layers present before the first up-sampling begins. The defining characteristic of proposed network is the use of max pooling indices in the decoders to perform up-sampling of low-resolution feature maps. This leads to keeping of the important detailed features in the image and non-useful features are erased. This neural

network provides smooth images without any post-processing technique involved. This method could outperform two FCN and Unet architectures.

FCN, despite up-convolutional layers and a few shortcut connections produces coarse segmentation maps. Therefore, more shortcut connections are introduced. However, instead of copying the encoder features as in FCN, indices from max-pooling are copied. This proposed method more memory-efficient than FCN. Also, in proposed method only the pooling indices are transferred to the expansion path from the compression path, using less memory. Whereas in the Unet, entire feature maps are transferred from compression path to expansion path making, using a lot of memory. Also, the outputs producing by this method are smooth and the borders between the region of interest and surrounded areas can't be detected precisely by the physicians, because of this we used a threshold technique for making the results sharper as post processing technique which is clarified in the next parts of this manuscript. The architecture of proposed neural network has been shown in Fig. 2.

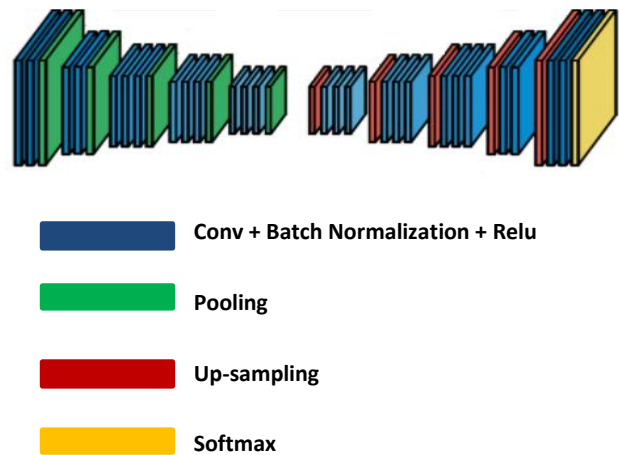


Fig. 2: Architecture of proposed neural network.

The architecture consists of a sequence of non-linear processing layers (encoders) and a corresponding set of decoders followed by a pixel-wise classifier. Typically, each encoder consists of one or more convolutional layers with batch normalization and a ReLU non-linearity, followed by non-overlapping max-pooling and sub-sampling.

The sparse encoding due to the pooling process is up-sampled in the decoder using the max-pooling indices in the encoding sequence. One key ingredient of this method is the use of max-pooling indices in the decoders to perform up-sampling of low resolution feature maps. This has the important advantages of retaining high frequency details in the segmented images and also

reducing the total number of trainable parameters in the decoders. The entire architecture can be trained end-to-end using stochastic gradient descent.

#### B. Loss Function

The loss functions used here are both Binary-crossentropy and Jaccard distance. The cross-entropy is a function which measures how far away from the true value the prediction is for each of the classes and then averages the errors class wise to obtain the final loss. In this problem, there lies only two classes for each pixel, either black or white (0 or 1) as per the mask. So, here binary cross-entropy is used as the loss function rather than the categorical cross-entropy originally proposed. The binary cross-entropy is in the below form:

$$l(y, \hat{y}) = -\frac{1}{N} \sum_{i=0}^N (y * \log(\hat{y}_i) + (1 - y) * (1 - (\hat{y}_i))) \quad (2)$$

Moreover, we have utilized Jaccard distance as loss function, but eventually we have reported our results based on binary cross entropy, because it had more accurate and higher evaluation metrics. Jaccard distance defines as following [16] :

$$d_j(M, C) = 1 - J(M, C) = 1 - \frac{|M \cap C|}{|M| + |C| - |M \cap C|} \quad (3)$$

M represents the ground truth of segmentation, which is normally a manually identified tumor region, and C represents a computer-generated mask.  $d_j(M, C)$  itself is not differentiable, which makes it difficult to be directly applied into backpropagation.

#### C. Network Training

For the training process, we have utilized 75% of 200 images that are available in the PH2 dataset [17]. moreover, the actual number of images in both PH2 dataset and Chest-Xray images are more than 150, because after image augmentation technique as preprocessing, the number of images increases to 450 and then enter to the network. We have separated these images into training and validation dataset for improving the network performance. 20% of these 450 image associate to validation dataset and the rest of them associate for training dataset. As per the architecture of the network the total parameters to be trained are 33,377,795 out of 33,393,669 whereas the non-trainable parameters are 15,874. The implementations are in Keras and the environment used is the google colab, cloud space for python codes.

#### D. Image Augmentation

The procedure of image augmentation on training images has been used for increasing the robustness of the model and reducing the chances of overfitting. Also, it will increase the images that are available in the

dataset. The two simple techniques that have been used in this method are image rotation and horizontal flipping [18].

In the image rotation, the images are rotated around the  $[-40, +40]$  degrees and for horizontal flip, the images are reversed around horizontal axis. All the above transformations are exactly performed on the corresponding masks of the images as well to maintain the correct orientation of feature images with their truth masks. As we have mentioned in the last part, after the augmentation the transformed images are included in the training set which increases our training set from 150 to 450. Out of these 450 images, 90 (20%) have been excluded from training set for the formation of a validation set and the rest of images associate to training dataset. Results of our image augmentation technique have been displayed in Fig. 3.

In the image augmentation technique, both original medical images and their corresponding masks have been affected by this technique and because of this, the total number of training images that are going to feed to the neural network, increase to 450.

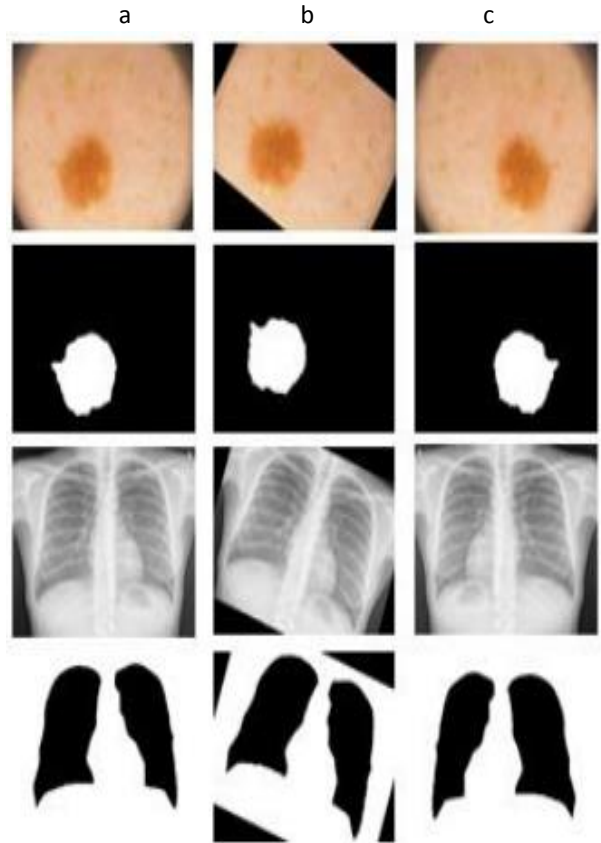


Fig. 3: image augmentation technique. a) original medical images with their corresponding masks. b) rotated images with their corresponding masks. c) horizontal flipped images with their corresponding masks.

#### E. Batch normalization

Batch normalization [14] is the technique of speeding

up the learning process of the neural network by normalizing the values in the hidden layers similar to the principle behind the normalization of the features in the data or activation values.

In the proposed network the batch normalization layer is presented after every convolution layer with a total of 25 batch normalization layers in the entire network architecture.

## Experimental Results and Design

### A. Datasets

The used medical datasets include PH2 dermoscopic dataset which contains 200 dermoscopic images and their label masks and Chest-Xray images that contains 200 RGB images and their corresponding label masks. The dimension of dermoscopic images is 572\*765 and the dimension of Chest-Xray images is 512\*512. The dataset has been provided publicly for experimental and studying purposes, to facilitate research on both segmentation and classification algorithms of medical images.

The PH2 dataset is acquired at the Dermatology Service of Hospital Pedro Hispano, Matosinhos, Portugal and Chest-Xray dataset has provided in Kaggle [19]. Before feeding the medical images to the network, we have two preprocessings that one of them is resizing the images for speeding up the neural network. In this work, we resize all of the medical images into 192\*256 and make them smaller.

It largely reduces the parameters to be trained in the network as well as the training time and complexity without significantly affecting the results. We train and evaluate our model with RGB 8 bit images and test it by label masks. The size of evaluation set is 20% of train set and the size of test set is 25% of the label masks set (50 images).

### B. Performance Evaluation

The outputs of the proposed neural network are binarized in to the lesion masks. The performance of the proposed algorithm has assessed by comparing computer generated masks as output with ground truths which are provided in the label masks dataset. We have assessed our model's performance by the following metrics:

### C. Jaccard Index (JA)

This metric also has known as Intersection Over Union.

The Jaccard similarity coefficient is a statistical similarity measurement to check the diversity among the sample sets.

The IOU gives the similarity among sets and the formula is the size of the intersection over the size of the union of the sets.

we can define evaluation metrics based on confusion matrix components.

Let TP, TN, FP, FN refer to the number of true positives, true negatives, false positives, and false negatives. We can show Jaccard distance by JA and define it as following formula:

$$JA = \frac{TP}{TP + FN + FP} \quad (4)$$

TP is the number of pixels that have been predicted as ROI correctly, FN is the number of pixels that have not been predicted as ROI wrongly and FP is the number of pixels that have been predicted as ROI wrongly.

### D. Dice Coefficient

The Dice score (F1 score) is like precision. It measures the positives as well as it applies penalty to the false positives given by the model.

It is more similar to precision than accuracy. We have shown dice coefficient by DI and have calculated it by the following formula:

$$DI = \frac{2 * TP}{(TP + FP) + (TP + FN)} \quad (5)$$

### E. Recall

Recall is a measure which is targeted towards the actual or the true positives yielded by the model output. In the scenarios where the cost of the False Negatives is greater than recall is the better metric to choose the best model among the possible ones. Recall also known as sensitivity (SE). we can calculate Recall as following formula:

$$SE = \frac{TP}{TP + FN} \quad (6)$$

### F. Accuracy

Accuracy approximates that how close our predicted output to the real ground truth. We have shown it by AC and have calculated it as following formula:

$$AC = \frac{TP + TN}{TP + FN + TN + FP} \quad (7)$$

## Comparison with Two Famous Architectures

Moreover, we have compared our results with two famous architectures, include Unet and FCN networks and the methods that have implemented in [16], [20]. We have shown our results in Table 1 by using PH2 dataset.

Also, we have implemented our method on Chest-Xray dataset to develop the algorithm on different medical images. We have shown our results by using

Chest-Xray medical images and compare it with other methods in [Table 2](#).

Table 1: Comparison results with other methods, based on different optimization algorithms, using PH2 dataset

Method	AC	DI	JA	SE
Yuan [16]	96.3	92.2	86.1	92.6
FCN	91.7	64.8	87.8	82.2
Unet	90.9	85.3	92.1	93
Our method	97.2	76.5	94.5	96.3

Table 2: comparison results with other methods, based on different optimization algorithms, using Chest-Xray dataset

Method	AC	DI	JA	SE
Johnatan [20]	96.97	93.56	88.07	97.54
FCN	91.16	87.03	92.90	98.31
Unet	88.87	88.90	93.11	92.84
Our method	97.78	97.33	98.38	99.26

As shown in the [Table 1](#) and [Table 2](#), our method has better results with higher evaluation metrics than the other methods that we have mentioned. We have compared our method with two Unet and FCN methods, because they have robust results in medical image segmentation and many works have done by these two methods.

## Results and Discussion

We have implemented our algorithm in the google colab space and finally, we have displayed our simulation results in [Fig. 5](#) and [Fig. 6](#). Our model is robust on blurry borders and segments the skin lesions clearly. We have implemented our final results in matlab2014 by implementing the segmentation results on their corresponding original medical images. The borders of region of interests (ROI) are clear in final results and doctors can recognize the ROI totally and cure the patients.

Moreover, we have implemented two FCN and Unet methods on our dataset, but as shown in [Fig. 4](#), the borders of ROI are blurry and not clear. Our method is a robust and precise algorithm toward medical image segmentation that can implement on other medical images like brain cancer dataset, bladder, Covid19-chest-xray medical images and etc.

we have shown each medical image with their segmentation result by this method and their final result. Firstly, we have displayed results for dermoscopic medical images in [Fig. 5](#). As mentioned before, we can observe in results that our method has more robust outputs than the other methods. The borders of ROI are clear and specialists can detect them totally. For dermoscopic images, there are lots of complex Region of Interests with illumination variations that our method could overcome these problems and segmented the legions in these images.

Also, for Chest-Xray images, there are illumination variations that our algorithm could overcome these problems too.

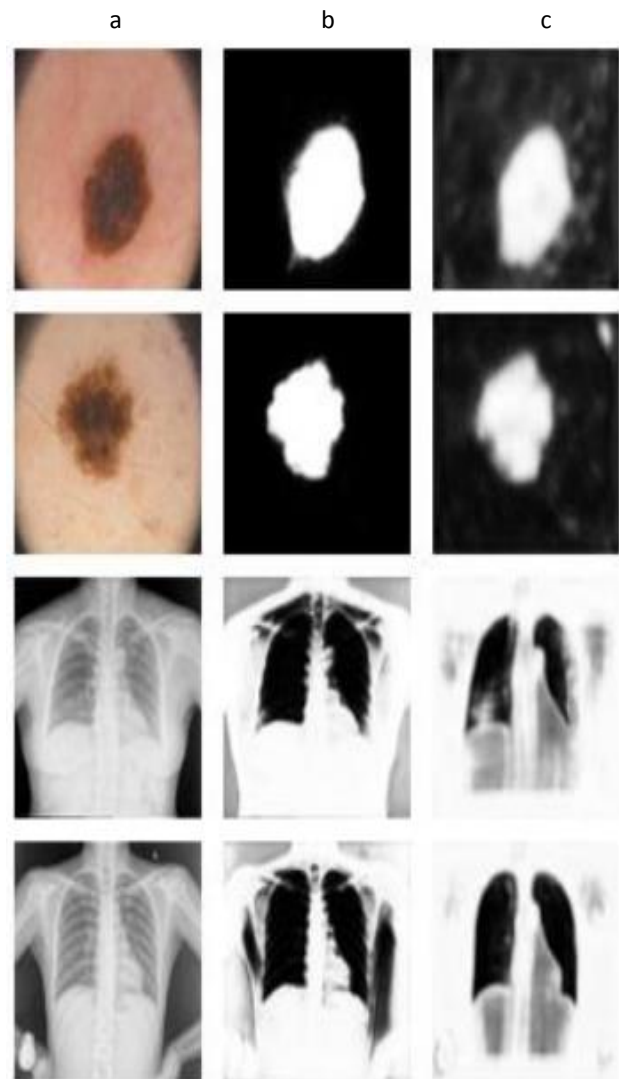


Fig. 4: Results of Unet and FCN. a) original medical images. b) Unet segmentation results. c) FCN segmentation results.

For Chest-Xray medical images, we have segmented and separated lung's texture from the other parts and also the Chest bone structures are clear in these images. By this work all of the problems including lung tumors,

lesions in lungs or Bone structure and also the infections in lungs and some diseases that happen by them like Covid19 can be detected completely. We have displayed the results for chest-Xray medical image segmentation in Fig. 6.

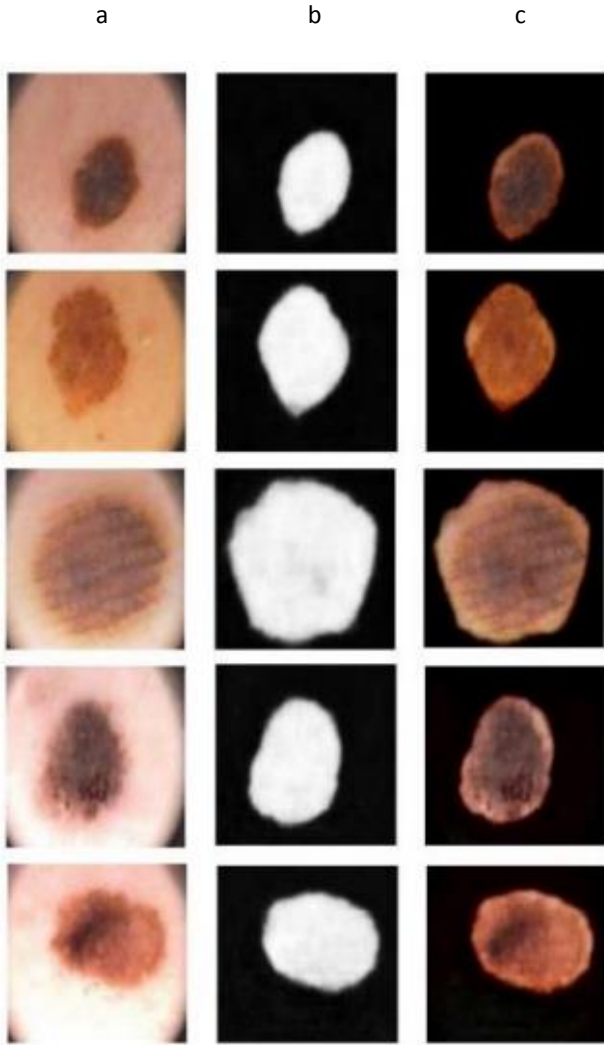


Fig. 5: Final simulation results. a) Original dermoscopic images. b) Segmentation outputs. c) Final results.

As results display, the proposed algorithm has better and more accurate results than Unet and FCN. The borders between lungs and other textures in segmented results are exactly as similar as original images. Also, in final results, we have implemented the segmentation of original images. We utilized a post-processing step in our algorithm that increases the resolution of segmented images and sharpens the borders between ROI and other regions by threshold technique. By this technique, we can compare the segmented outputs with their corresponding binary masks and evaluate the performance of our algorithm by observation too. We have shown the post-processed outputs in Fig. 7.

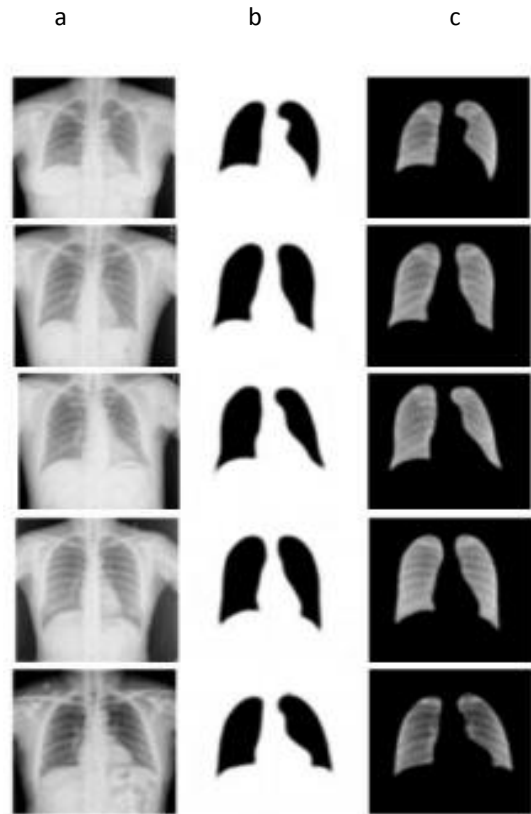


Fig. 6: Final simulation results. a) original chest-Xray images. b) segmentation outputs. c) final results.



Fig. 7: post-processed outputs. a) binary masks as ground truths. b) corresponding segmented outputs of each binary mask after post-processing.

## Conclusion

In this work, we proposed an algorithm based on deep convolutional neural networks for medical image segmentation on dermoscopic and Chest-Xray medical images. Several effective training strategies were implemented to tackle the challenges that training a deep network may face when only limited training data is available.

We designed our loss function based on both Jaccard distance and binary-crossentropy. Two techniques of image augmentation, image rotation and horizontal flipping on the training dataset are performed before feeding it to the network for training. After the training process the model was evaluated on several measures for statistical values.

The predictions produced from the model on test images were postprocessed using the threshold technique to remove the blurry boundaries around the predicted lesions and make images sharper for better detection.

As shown in [Table 1](#) and [Table 2](#), Our approach could outperform the state-of-the-art methods like Unet and FCN or the algorithms that have been done in [16], [20] when evaluating on an open challenge dataset of Skin Lesion Analysis Towards Melanoma Detection in PH2 and Chest-Xray medical images. We have displayed our final results in [Fig. 5](#), [Fig. 6](#) and it has demonstrated clearly that the proposed method is robust to various image artifacts and imaging acquisition conditions while using minimum pre- and post-processings. We believe this method can generalize well to other medical image segmentation tasks.

We hope future works will develop our method for dice coefficient improvement and implement it on other famous datasets, like: ISIC2017 [21] and ISBI2016 [22] and also the other medical datasets for different parts of the body.

## Author contributions

M.Taheri and M.Rastgarpour conceived of the presented idea. M.Taheri developed the theory and performed the computations. M.Rastgarpour and A.Koochari verified the analytical methods. M.Rastgarpour encouraged M.Taheri to investigate and supervised the findings of this work. All authors discussed the results and contributed to the final manuscript.

## Acknowledgment

The authors are thankful to the dermatology service of Hospital Pedro Hispano in Portugal, who makes the 11 dermoscopic image data available. They also thank the anonymous reviewers whose comments and suggestions helped improve this manuscript. Also, we are thankful to

Kaggle website that has provided so many different datasets that are available for researches and programmers.

## Conflict of Interest

The authors declare no potential conflict of interest regarding the publication of this work. In addition, the ethical issues including plagiarism, informed consent, misconduct, data fabrication and, or falsification, double publication and, or submission, and redundancy have been completely witnessed by the authors.

## Abbreviations

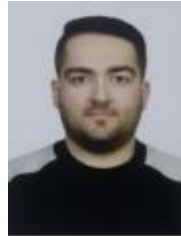
<i>CNN</i>	Convolutional Neural Network
<i>SGD</i>	Stochastic Gradient Descent
<i>FCN</i>	Fully Convolutional Neural Network
<i>ROI</i>	Region Of Interest
<i>JA</i>	Jaccard Index
<i>DI</i>	Dice Coefficient
<i>SE</i>	Sensitivity
<i>AC</i>	Accuracy
<i>IOU</i>	Intersection Over Union
<i>TP</i>	True Positive
<i>TN</i>	True Negative
<i>FP</i>	False Positive
<i>FN</i>	False Negative

## References

- [1] J.U. Kim, H.G. Kim, Y.M. Ro, "Iterative deep convolutional encoder-decoder network for medical image segmentation," presented at the 2017 39th Annual International Conference of the IEEE Engineering in Medicine and Biology Society (EMBC), Seogwipo, South Korea, 2017.
- [2] Y. Chang et al., "Automatic segmentation and cardiopathy classification in cardiac MRI images based on deep neural networks," presented at the 2018 IEEE International Conference on Acoustics, Speech and Signal Processing (ICASSP), Calgary, AB, Canada, 2018.
- [3] A. Işın, C. Direkoğlu, M. Şah, "Review of MRI-based brain tumor image segmentation using deep learning methods," *Procedia Comput. Sci.*, 102: 317-324, 2016.
- [4] P. Moeskops et al., "Deep learning for multi-task medical image segmentation in multiple modalities," in *Proc. International*

- Conference on Medical Image Computing and Computer-Assisted Intervention, 468-486, 2016.
- [5] D. Abdelhafiz et al., "Convolutional neural network for automated mass segmentation in mammography," presented at the 2018 IEEE 8th International Conference on Computational Advances in Bio and Medical Sciences (ICCABS), Las Vegas, NV, USA, 2018.
- [6] H. Fu et al., "Retinal vessel segmentation via deep learning network and fully-connected conditional random fields," Presented at the 2016 IEEE 13th international symposium on biomedical imaging (ISBI), Prague, Czech Republic, 2016.
- [7] Z. Guo et al., "Deep learning-based image segmentation on multimodal medical imaging," *IEEE Trans. Radiat. Plasma Med. Sci.*, 3(2): 162-169, 2019.
- [8] M. Emre Celebi, Q. Wen, S. Hwang, H. Iyatomi, G. Schaefer, "Lesion border detection in dermoscopy images usingensembles of thresholding methods," *Skin Res. Technol.*, 19(1): e252– e258, 2013.
- [9] H. Zhou, X. Li, G. Schaefer, M.E. Celebi, P. Miller, "Meanshift based gradient vector flow for image segmentation," *Comput.Vis. Image Understand.*, 117(9): 1004–1016, 2013.
- [10] F. Xie, A.C. Bovik, "Automatic segmentation of dermoscopy images using self-generating neural networks seeded by genetic algorithm," *Pattern Recognit.*, 46(3): 1012–1019, 2013.
- [11] T. Mendonça et al., "PH 2-A dermoscopic image database for research and benchmarking," presented at the 2013 35th annual international conference of the IEEE engineering in medicine and biology society (EMBC), Osaka, Japan 2013.
- [12] S. Pereira, A. Pinto, V. Alves, C.A. Silva, "Brain tumor segmentation using convolutional neural networks in MRI images," *IEEE Trans. Med. Imag.*, 35(5): 1240–1251, 2016.
- [13] Y. LeCun, L. Bottou, Y. Bengio, P. Haffner, "Gradientbased learning applied to document recognition," in *Proc. the IEEE*, 6(11): 2278–2324, 1998.
- [14] S. Ioffe, C. Szegedy, "Batch Normalization: Accelerating Deep Network Training by Reducing Internal Covariate Shift," in *Proc. the 32nd International Conference on Machine Learning, PMLR*, 37:448-456, 2015.
- [15] T. Zhang "Solving large scale linear prediction problems using stochastic gradient descent algorithms" presented at the 21th International Conference on Machine Learning, Banff, Canada, 2004.
- [16] Y. Yuan, M. Chao, Y.C. Lo, "Automatic skin lesion segmentation using deep fully convolutional networks with jaccard distance," *IEEE Trans. Med. Imaging*, 36(9): 1876-2017.
- [17] M.H. Jafari, E. Nasr-Esfahani, N. Karimi, S. Soroushmehr, S. Samavi, K. Najarian, "Extraction of skin lesions from nondermoscopic images using deep learning," *arXiv preprint arXiv: 1609.02374*, 2016.
- [18] M. Avendi, A. Kheradvar, H. Jafarkhani, "A combined deeplearning and deformable-model approach to fully automatic segmentation of the left ventricle in cardiac MRI," *Med. Image Anal.*, 30: 108–119, 2016.
- [19] <https://www.kaggle.com/search?q=Chest+xray+segmentation>
- [20] J. Carvalho Souza, J.O.B. Diniz, J.L. Ferreira, G.L. Franc, a da Silva, A. Corr'ea Silva, A. Cardoso de Paiva, "An automatic method for lung segmentation and reconstruction in chest X-Ray using deep neural networks," *Comput. Methods Programs Biomed.*, 177: 285-296, 2019.
- [21] D. Gutman, N.C.F. Codella, E. Celebi, B. Helba, M. Marchetti, N. Mishra, A. Halpern, "skin lesion analysis toward melanoma detection: A challenge at the 2017 International Symposium on Biomedical Imaging (ISBI), Hosted by the International Skin Imaging Collaboration (ISIC)," presented at the 2018 IEEE 15th International Symposium on Biomedical Imaging (ISBI), Washington, DC, USA, 2018.
- [22] D. Gutman, N.C.F. Codella, E. Celebi, B. Helba, M. Marchetti, N. Mishra, A. Halpern, "Skin lesion analysis toward melanoma detection: A challenge at the International Symposium on Biomedical Imaging (ISBI) 2016, hosted by the International Skin Imaging Collaboration (ISIC)," May 2016.

## Biographies



**Mohammad Taheri** was born in 1994 in the Damghan city of Semnan province, Iran. He received his B.Sc. degree in information technology engineering from Semnan university, Semnan, Iran, M.Sc degree in Artificial intelligence from Islamic Azad university, Science & Research branch, Tehran, Iran in 2018 and 2020, respectively. His major interests include image processing, computer vision, medical image segmentation, deep neural networks, convolutional neural networks and machine learning.



**Maryam Rastgarpour** received her B.Sc. in software engineering from Kharazmi university, Tehran, Iran, in 2003, M.Sc. and Phd degrees in computer engineering: AI from Islamic Azad University (IAU), Science & Research branch, Tehran, Iran, in 2014. She is currently an assistant professor in the department of Computer engineering at the Islamic Azad University, Saveh branch, Saveh, Iran. Her research interests include in the areas of Machine Vision, Optimization, Data Mining and expert systems specifically in medical image segmentation. She has supervised or advised over 60 MS theses or PhD dissertations and contributed or coauthored more than 60 papers published in journals or conference records or as book chapters.



**Abbas Koochari** received his B.Sc. in Computer Engineering from Shahed University, Tehran, Iran, M.Sc. degree in Computer Engineering: AI from the Amirkabir University of technology, Tehran, Iran and Ph.D. degree in Computer Engineering: AI from the Iran University of Science and technology, Tehran, Iran. He is currently an assistant professor in the department of computer engineering at the Islamic Azad University, Science & Research Branch, Tehran, Iran. His research interests include Signal Processing, Speech Recognition, Image and Video Processing.

**Copyrights**

©2021 The author(s). This is an open access article distributed under the terms of the Creative Commons Attribution (CC BY 4.0), which permits unrestricted use, distribution, and reproduction in any medium, as long as the original authors and source are cited. No permission is required from the authors or the publishers.



**How to cite this paper:**

M. Taheri, M. Rastgarpour, A. Koochari, "A novel method for medical image segmentation based on convolutional neural networks with SGD optimization," *J. Electr. Comput. Eng. Innovations*, 9(1): 37-46, 2021.

**DOI:** [10.22061/JECEI.2020.7404.390](https://doi.org/10.22061/JECEI.2020.7404.390)

**URL:** [http://jecei.sru.ac.ir/article\\_1482.html](http://jecei.sru.ac.ir/article_1482.html)

